CHEMICAL ENGINEERING TRANSACTIONS
VOL. 92, 2022
A publication of AIDIC
The Italian Association of Chemical Engineering
Online at www.cetjournal.it
Guest Editors: Rubens Maciel Filho, Eliseo Ranzi, Leonardo Tognotti

ISBN 978-88-95608-90-7; **ISSN** 2283-9216
DOI: 10.3303/CET2292059

Mixing in Biogas Fermenters: Experimental Characterization of a Scale-Down Geometry

Federico Alberini, Francesco Maluta, Alessandro Paglianti, Giuseppina Montante*

Department of Industrial Chemistry "Toso Montanari", Laboratory of Applied Fluid Dynamics and Mixing - Alma Mater Studiorum – Università di Bologna, via Terracini 34, 40131 Bologna, Italy
giuseppina.montante@unibo.it

In this work, the fluid dynamics features of a real industrial configuration of a biogas fermenter, which consists in a cylindrical tank stirred with three top-entering shafts with multiple impellers, are investigated. The analysis is based on the experimental characterization of a laboratory model digester of 0.49 m in tank diameter obtained from the scale-down based on the geometrical similarity criterion of a full-scale digester of diameter equal to 17 m. The aim of the work is to evaluate the appropriateness of the design for the requirements of the biogas production process and to suggest possible improvements to the overall mixing operation.
The fluid dynamics investigation is carried out using either water or an aqueous solution of xanthan gum, in order to assess the impact of the variation of the rheological properties at different impeller speeds and direction of rotation of the impellers on the mixing features. To this end, Particle Image Velocimetry is adopted to obtain the velocity fields for the different liquid phases. The data analysis allows to identify possible critical fluid dynamics characteristics that may affect the fermentation, as for example the presence of stagnant zones, where sinking layers might be expected, thus explaining the failure of the biogas production often observed in the biogas production plant.

1. Introduction

The production of biogas from the fermentation of organics by anaerobic digestion is increasingly adopted in several countries. It already effectively contributes to the production of renewable energy and its development requires integration of different fields, going from biogas process to energy system modelling (Heiker et al., 2021). Among the challenges in biogas process research, the optimization of the mixing system and the reliability of scale-up criteria are particularly important, being the selection of the agitation system and the agitation rate critical to achieve high production rate (Lebranchu et al., 2017). The evolving rheology in the fermenter and the sedimentation and flotation of the feedstock pose additional issues that must be tackled with appropriate mixing system design (Dapelo et al. 2015).
The optimization of the digester design and of the operating conditions is expected to improve the overall performance and to reduce the energy requirements of biogas production, being stirring responsible for up to 54% of the power consumption of current biogas plants (Kowalczyk et al., 2013). Attainment of complete solid distribution (Kaparaju et al., 2008) and perfect mixing (Keshtkar et al., 2003) are often assumed for continuously stirred digesters, while strong variations always occur particularly at industrial scale. The most common reactor types employed for wet fermentation are vertical stirred tanks provided with mechanical agitators (Weiland, 2010). Often, single or multiple stirrers much smaller than the tank diameter are adopted for mixing unbaffled tanks of low aspect ratio, that is an unconventional stirred tank configuration. Generally, in the literature, the local hydrodynamic characteristics of the digesters are scarcely investigated by experimental methods (Montante and Paglianti, 2015). Moreover, the knowledge on the fluid mixing of unconventional reactor geometries is relatively scarce. Thus, the hydrodynamics characterization of a real digester design is expected to contribute to identifying reliable design rules and scale up criteria.

Paper Received: 4 January 2022; Revised: 4 March 2022; Accepted: 5 May 2022
Please cite this article as: Alberini F., Maluta F., Paglianti A., Montante G., 2022, Mixing in Biogas Fermenters: Experimental Characterization of a Scale-down Geometry, Chemical Engineering Transactions, 92, 349-354 DOI:10.3303/CET2292059

2. Experimental

The investigation was carried out in a Perspex stirred tank shown in Figure 1a of total volume equal to 47 L, obtained from the scale down of an industrial digester of total filled volume equal to about 1500m^3 by applying the criterion of geometrical similarity. The flat-bottomed cylindrical vessel, of diameter T equal to 49 cm and height, H, equal to T/2, was closed with a lid on top. The scaled-down liquid level, H_L, was always maintained at 0.38T. Agitation was provided with multiple blades (Figure 1b) fixed to three top-entering shafts set symmetrically respect to the vessel axis at a radial distance of 170 mm from the centre. The blades had total length equal to 0.04T. The three shafts are equipped with 6 blades each, thus resulting in 18 blades, that in the full scale fermenter were often used intermittently. When the shafts rotated clockwise the inclination of the three lowest blades provided up-pumping agitation, while the three highest provided down-pumping agitation, and vice versa when the shaft rotated anticlockwise.
The experiments were carried out at the impeller rotational speed, N, of 133rpm, that corresponds to the impeller speed of 12.5rpm adopted in the industrial condition applying the constant power consumption scale-down criterion, that results in maintaining constant N^3D^2 at the different scales. Also, a 50% lower value (67rpm) and a 63% higher value (217rpm) with respect to the constant specific power consumption impeller speed were considered. The constant Reynolds number (constant ND^2) and the constant tip speed criteria (constant ND), corresponding to 15170rpm and 435rpm, respectively, were instead discarded. Demineralized water and an aqueous solution of xanthan gum (Xa) with a concentration of 1g per kg of water were adopted.

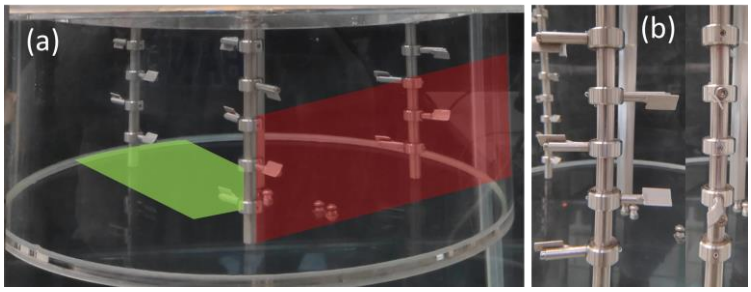

Figure 1: (a) Scale down biogas fermenter used for the PIV experiments, highlighted the horizontal plane (green) and the vertical plane (red); (b) side and front view of the impellers.

2.1 The Particle Image Velocimetry measurement

The liquid velocity field was determined in different vertical and horizontal sections of the vessel using the Particle Image Velocimetry (PIV). The flow was seeded with silver-coated hollow glass particles of mean diameter equal to 10 μm and was illuminated with a light sheet approximately 2 mm thick. The light source was a pulsed Nd:YAG laser (light wavelength equal to 532 nm, frequency equal to 15 Hz, energy of 65 mJ/pulse) provided with a cylindrical lens for the light sheet generation. The image acquisition was performed by a digital HiSenseMKII camera (1344×1024 pixels CCD) placed perpendicular to the laser sheet and provided with an optical filter to cut the ambient light. The laser light refractive effects at the curved vessel surface were minimized, since the vessel was placed in a Perspex square cross-section tank filled with the working liquid similarly to previous investigations of bioreactors for different applications (Montante et al., 2013). The laser control, the laser/camera synchronization and the data acquisition and processing were handled by a Dantec Dynamics system.
To guarantee a sufficient spatial resolution, the measurement areas were limited to sections of the measurement planes, as shown in Figure 1. The mean axial, radial, and tangential velocity components, U, V and W, are positive if directed toward the vessel wall, upwards and in the same direction of the impeller rotation, respectively. The selection of the measurement parameters was performed with the usually adopted criteria for the PIV experimental error minimization (Montante and Paglianti, 2014). The time interval between two laser pulses was varied in the range 800-3800 μs, depending on the impeller speed and the fluid, in order to maintain the particle displacement below 25% of the length of the interrogation area size. The velocity vectors were calculated by applying a cross-correlation algorithm to each image pair on a rectangular grid with 50% overlap between adjacent cells and an interrogation area of 32×32 pixel. The resulting vector resolution was of about 2.3mm in the horizontal plane and 1.7mm in the vertical plane. The instantaneous vectors were submitted to a validation procedure based on the evaluation of the peak heights in the correlation plane and of velocity magnitude. The vectors that did not satisfy the selected validation criteria were discarded. The number of image

pairs collected in each run was equal to 1000 and at least 500 image pairs were required to obtain statistical convergence on mean velocities.

2.2 Rheological and flow regime characterization

The rheological measurements have been carried out using a Anton Paar Physica MCR301 rotational rheometer. The geometry used for the flow curve characterization is stainless steel hollow bob B-DG26 and cup C-DG26/SS for measurement according to DIN 54453. The range of shear rate for the flow ramp has been selected between 0.1- 500 s^{-1} to ensure investigation of the full range of interest for the stirred vessel at selected configurations. Measurement showed that effects of temperature differences in the range 20-30°C were minimal at the shear rates of interest, as shown in Figure 2, where the red lines correspond to the shear of interest for the three selected impeller speeds.

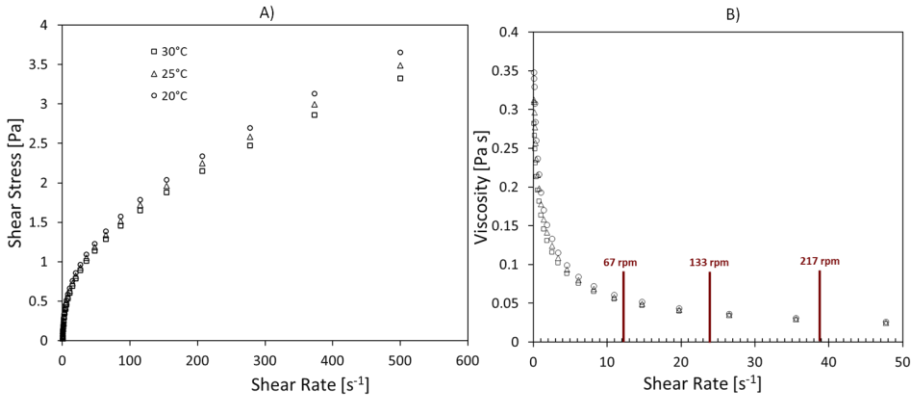

Figure 2: Flow curve (A) and viscosity vs shear rate (B) at three different temperatures for the water-Xanthan gum solution 1 gr L^{-1}.

The apparent viscosity, μ_a, was estimated adopting the Metzner-Otto method as:

$$\mu_a = k_s \dot{\gamma}^{n-1} \quad (1)$$

$$\dot{\gamma} = KN \quad (2)$$

where k_s is the consistency index, $\dot{\gamma}$ the shear rate and n the flow behavior index. These indexes are into the range of typical digester fluids (Annas et al., 2019) and similar solutions were adopted also recently by Kolano et al. (2021) in the investigation of a pilot biogas fermenter equipped with side-entering impellers. For the constant K, the value of 11 was adopted, as recommended for high speed impellers. The resulting values of μ_a were 0.05, 0.03, 0.025 Pa·s for N equal to 67 (1.11 rps), 133 (2.2 rps) and 217 (3.6rps) rpm, respectively. Therefore, in the investigated conditions, the rotational Reynolds number, that is defined as:

$$Re = \frac{\rho N D^2}{\mu} \quad (3)$$

ranges from 6.4×10^4 to 2.1×10^5 in water and from 1.3×10^3 to 8.3×10^3 in the Xa solution.

3. Results

In the following, the results obtained with the two fluids at different impeller speeds are compared and discussed. In addition to the conventional clockwise rotation, agitation was also performed with anticlockwise rotation, thus changing the agitation mode provided by the inclined blades. The corresponding variations of the liquid flow patterns are of special interest, in order to evaluate the possible improvement of the solid suspension characteristics, being this a critical aspect during the industrial operation. A preliminary visual estimation of the appropriateness of the impeller rotational speed scale-down criterion and on the difference obtained with clockwise and anticlockwise rotation mode is possible observing the pictures of the vessel shown in Figure 3a-b, where the biomass distribution at N=133rpm (same specific power of the industrial scale) close to the wall can be observed in the two cases. In order to reproduce the industrial conditions, the feedstock was added to the liquid from the corresponding top position of the feeding. The presence of the solid deposition confirms that the specific power consumption is the best among the available scale-down criteria for reproducing the industrial digester functioning, while at N=435 rpm (constant tip speed, not shown for brevity), complete suspension was

observed, that does not reproduce the industrial condition where significant solid deposition was detected at the impeller speed of 12.5rpm (133rpm in the constant specific power consumption scale down version).

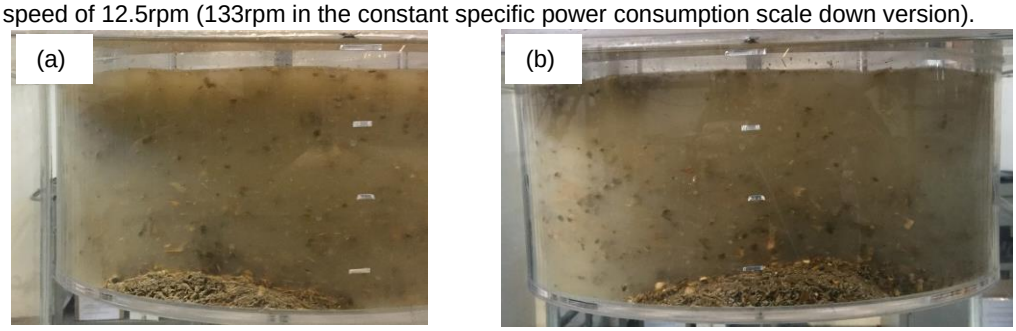

Figure 3: Visual observation of the feedstock distribution at N=133rpm, (a) clockwise impeller rotation; (b) anticlockwise impeller rotation.

In addition, the impeller rotation direction affects the solid distribution characteristics, as highlighted in Figure 3a-b from the different position of the solids on the vessel bottom. It is worth noticing that failure of the industrial digester was often caused by the presence of a pile under the feeding nozzle, therefore the movement of the settled solid may be crucial for process operation.

3.1 The liquid flow pattern

To verify how the different rotation directions affect the hydrodynamics of the system, the mean velocity fields were collected at the same impeller speed for the two directions. As a reference, the axial velocity colour maps on a vertical section of the vessel close to one of the shafts (as highlighted in Figure 1) are presented in Figure 4. The axial velocity is selected since it is the main responsible for the solid suspension from the tank bottom.

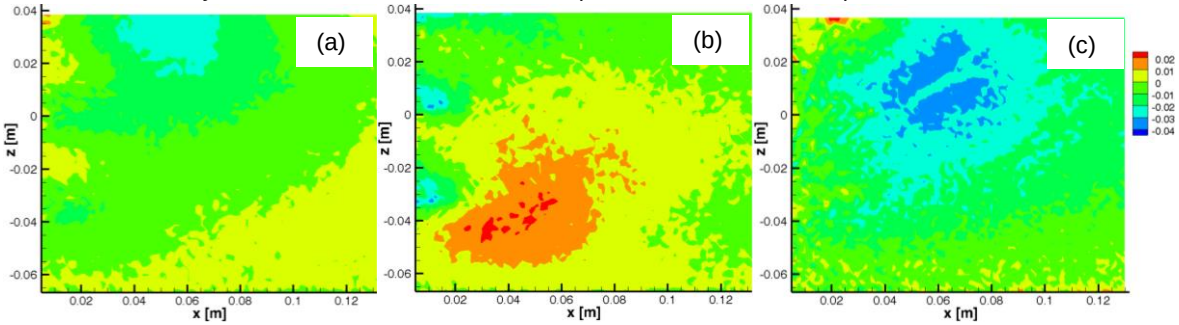

Figure 4: Mean axial velocity on a vertical section at N=133rpm. (a) water, clockwise impeller rotation, (b) water, anticlockwise impeller rotation, (c) Xa solution, clockwise impeller rotation. The colour scale is in m s^{-1}.

As it can be seen, the axial velocity magnitude exhibits a different distribution with the two different rotation directions and with different fluids. In particular, higher upwards axial velocity magnitude is obtained in water in the case of anticlockwise rotation (Figure 4b) with respect to the clockwise rotation (Figure 4a). Surprisingly, in the more viscous system (Figure 4c), higher absolute values of the axial velocity magnitude are observed in the middle of the section, thus highlighting the complexity of the hydrodynamics probably due to the different impellers discharge flow interaction. Overall, the velocity field shows the importance of optimizing the configuration, given that the main task of the agitation system is the distribution of the biomass in the whole vessel volume, trying at the same time to avoid the sedimentation of the solids.

The distributions of the radial and tangential velocities divided by the impeller tip speed (V_{tip}) on the horizontal section close to the tank bottom show a bimodal spread of both the components for the three investigated impeller speeds. Unsurprisingly for the middle and higher N values, the distributions match closely (Figure 5b,c and Figure 6b,c). This is simply explained by the Re numbers for the two aforementioned runs which can be considered both within the turbulent regime. On the contrary for the lower N, the rotational Reynolds number (Figures 5a and 6a) is typical of the high transitional regime, thus explaining the larger differences compared to the other two.

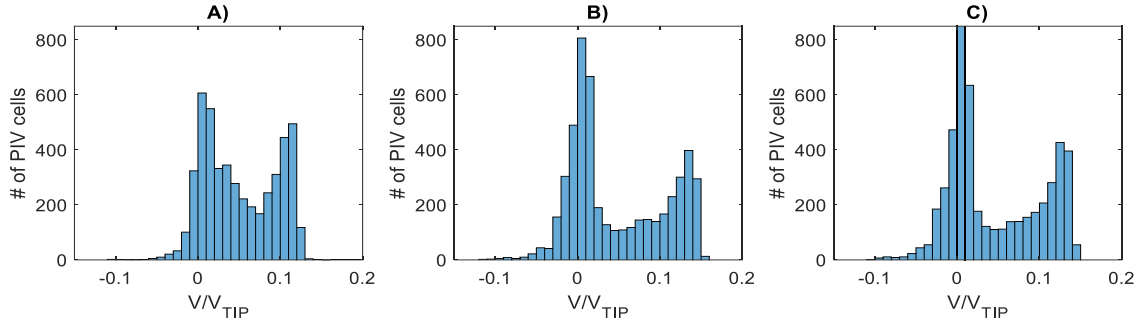

Figure 5: Dimensionless radial velocity distribution on a horizontal section close to the vessel bottom (z=1.5cm). Water: (a) N=67rpm; (b) N=133rpm, (c) N=217 rpm.

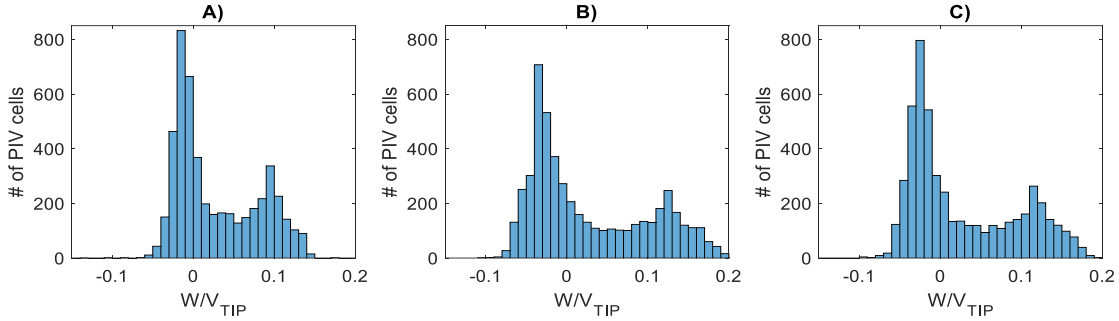

Figure 6: Dimensionless tangential velocity distribution on a horizontal section close to the vessel bottom (z=1.5cm). Water: (a) N=67rpm; (b) N=133rpm, (c) N=217 rpm.

On the other hand, different trends are observed in Figures 7 and 8 where similar plots are observed for the water solution of Xa, for the same PIV measurements region of interest (ROI). The different rheological behaviour of the fluid changes drastically the shape of the distributions. In this case, the distributions are mono-modal and generally the velocity intensity is within 5% of V_{tip}, compared to the just water case, where the velocity in the ROI reached 15% and 20 % of the tip speed respectively for the radial and tangential velocity. Concerning the relative shape of the distributions, increasing the impeller speed, for both radial and tangential velocity, the distributions assume a different shape and the similar shape cannot be observed for the middle and higher values of N, as seen for the water case. This is explained by the rheological flow map shown in Figure 2. For the Xa solution used for this work, despite the tip speeds are comparable to the previous cases, the apparent viscosities at different N are few orders higher in magnitude compared to the viscosity of water. If the values of apparent viscosities are used to calculate the Re numbers for the three runs for the Xanthan gum fluid, it is observed that at higher N the value of Re is less than 10^3. This suggests that the system, for the different operating conditions, is in low/middle transitional regime. This finding is very relevant if contextualized for a real biological reactor, such as a digester. Since the fluid rheology is more likely to be closer to the Xa solution used in this work, rather than that of water. This is important when initial considerations for digester design are made.

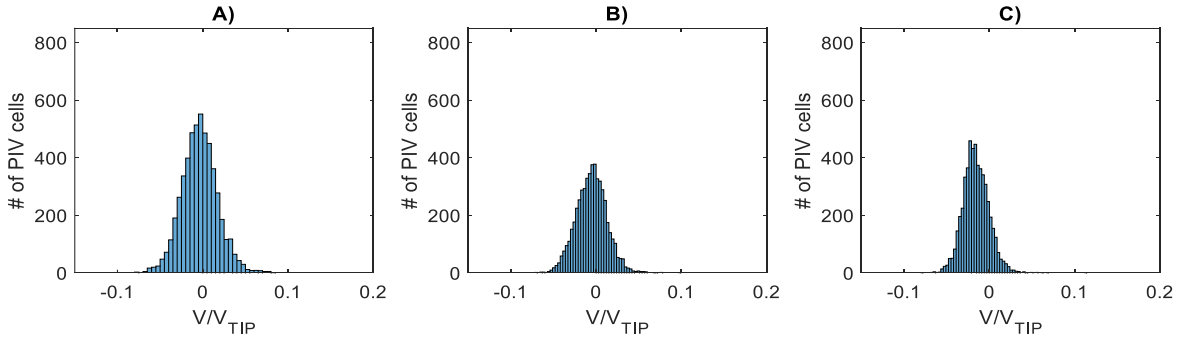

Figure 7: Dimensionless radial velocity distribution on a horizontal section close to the vessel bottom (z=1.5cm). Xa solution: (a) N=67rpm; (b) N=133rpm, (c) N=217 rpm.

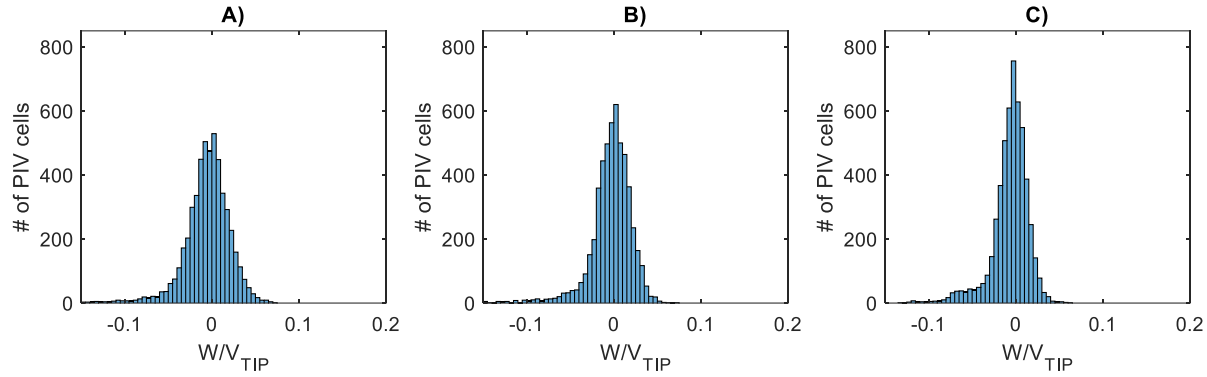

Figure 8: Dimensionless tangential velocity distribution on a horizontal section close to the vessel bottom (z=1.5cm). Xa solution: (a) N=67rpm; (b) N=133rpm, (c) N=217 rpm.

Firstly, underestimating the apparent viscosity, the power consumed by the motor will be drastically underestimated. Secondly, the complexity of the flow field will be difficult to predict using standard design approaches, particularly in the transitional regime. In fact, using a scale down experimental system is the only way to provide valuable and reliable information about the dynamics of a such complex system.

4. Conclusions

The verification of the scale-down criterion for the impeller speed and the evaluation of the effect of the operating mixing mode on the biomass suspension features suggests that for full scale design of biogas digester investigation of down-scale geometries can be particularly important for avoiding failure of the production plant particularly due to lack of distribution of the solid feedstock adopted in the process. As a difference with the case of conventional stirred tanks operating in fully turbulent regime, for this reactor configuration, the shape of the discharge flow of the impellers and their interaction exhibits significant differences depending on the Reynolds number.

References

Annas, S., Elfering, M., Volbert, N., Jantzen, H.-A., Scholz, J., Janoske, U., 2019, Influence of the Agitator Position on the Mixing Process in Biogas Plants Using Paddle Agitators, Chemie-Ingenieur-Technik, 91, 969-979.

Dapelo, D., Alberini F., Bridgeman J., 2015, Euler-Lagrange CFD modelling of unconfined gas mixing in anaerobic digestion, Water Research,85: 497-511

Heiker, M., Kraume, M., Mertins, A., Wawer, T., Rosenberger, S., 2021, Biogas plants in renewable energy systems-a systematic review of modeling approaches of biogas production Applied Sciences, 11, art. no. 3361

Kaparaju, P., Buendia, I., Ellegaard, L., Angelidakia, I., 2008, Effects of mixing on methane production during thermophilic anaerobic digestion of manure: Lab-scale and pilot-scale studies, Bioresour. Technol. 99, 4919-4928.

Keshtkar, A., Meyssami, B., Abolhamd, G., Ghaforian, H., Asadi, M.K., 2003, Mathematical modeling of non-ideal mixing continuous flow reactors for anaerobic digestion of cattle manure. Bioresour. Technol. 87, 113-124.

Kolano, M., Danke, J., Kraume, M., 2021, Using thrust to control the mixing process in stirred tanks with side-entering agitators and viscoelastic fluids, Biomass and Bioenergy, 152, art. no. 106180.

Kowalczyk, A., Harnisch, E., Schwede, S., Gerber, M., Span, R., 2013, Different mixing modes for biogas plants using energy crops. Appl. Ener., 112, 465-472.

Lebranchu, A., Delaunay, S., Marchal, P., Blanchard, F., Pacaud, S., Fick, M., Olmos, E., 2017, Impact of shear stress and impeller design on the production of biogas in anaerobic digesters, Bioresource Technology, 245, 1139-1147.

Montante, G., Paglianti, A., 2014, Hydrodynamics of a model stirred anaerobic digester, Chemical Engineering Transactions, 38, 49-54.

Montante, G., Paglianti, A., 2015, Fluid dynamics characterization of a stirred model bio-methanation digester, Chemical Engineering Research and Design, 93, 38-47.

Montante, G., Magelli, F., Paglianti, A., 2013, Fluid-dynamics characteristics of a vortex-ingesting stirred tank for biohydrogen production Chemical Engineering Research and Design, 91, 2198-2208.